

# Characterization of recycled styrene butadiene rubber ground tire rubber: Combining X-ray fluorescence, differential scanning calorimetry, and dynamical thermal analysis for quality control

Huan Liang,<sup>1,2</sup> Denis Rodrigue,<sup>1,3</sup> Josée Brisson<sup>1,2</sup>

<sup>1</sup>CERMA (Centre de recherche sur les matériaux avancés) and CQMF (Centre québécois sur les matériaux fonctionnels), Université Laval, Quebec City, Quebec, Canada G1V 0A6

<sup>2</sup>Department of Chemistry, Faculté des sciences et de génie, Université Laval, Quebec City, Quebec, Canada G1V 0A6

<sup>3</sup>Department of Chemical Engineering, Faculté des sciences et de génie, Université Laval, Quebec City, Quebec, Canada G1V 0A6

Correspondence to: J. Brisson (E-mail: josee.brisson@chm.ulaval.ca)

**ABSTRACT:** Appraisal of the main rubber characterization techniques for styrene butadiene rubber (SBR) was performed on standard SBR samples as well as recycled ground tire rubber (GTR) from an industrial tire recycling facility, containing a blend of SBR and natural rubber. The aim of the work was to provide additional information relevant to quality control in the field of rubber recycling. Benchmark characterization of industrial samples by inductively coupled plasma optical emission spectrometry, atomic absorption spectrometry, solid-state proton nuclear magnetic resonance, and elemental (CHNS) analysis are reported. X-ray fluorescence spectrometry is shown to be rapid and quantitative for determining the zinc content in an industrial context. Thermogravimetric analysis, already used to determine carbon black and inorganic material content in rubbers and GTR, is recommended for determination of monomer weight ratios of SBR sources not containing other rubbers, but not for GTR. Differential scanning calorimetry (DSC) measurements of the glass-transition show that changes in monomer ratio affect glass-transition temperature values, and therefore, DSC can be used to detect changes in rubber composition from batch to batch. These results show that DSC and X-ray fluorescence spectroscopy characterization techniques can be used for GTR and may lead to more thorough and rapid quality control procedures of these complex samples. © 2015 Wiley Periodicals, Inc. *J. Appl. Polym. Sci.* **2015**, *132*, 42692.

**KEYWORDS:** differential scanning calorimetry; recycling; rubber; thermal properties; X-ray

Received 4 March 2015; accepted 29 June 2015

DOI: 10.1002/app.42692

## INTRODUCTION

The increasing number of cars worldwide results in an increase in used tires. Their storage causes environmental and safety problems, and reprocessing and reuse of these tires in an economically viable way constitutes an important challenge.<sup>1</sup>

In 2003, it was estimated that around 290 million scrap tires were generated in the United States alone.<sup>2</sup> The tire sole accounts for about a half of each car tire, and is a blend of 10%–40% styrene butadiene rubber (SBR) with natural rubber (mainly composed of polyisoprene units). Depending on their use (all-season, all-terrain, high performance, snow, mud, SUV, truck, etc.) and manufacturer, various polymer compositions and additives are found in tires: sulfur is added for vulcanization, zinc oxide (ZnO) is added for activation, silica and calcium carbonates are used as fillers, etc.<sup>3</sup> In addition,

reinforcement (steel bead wire, thermoplastic or natural polymer cord, etc.) are also imbedded in the rubber sole.

During the recycling process, tires are ground into a coarse powder, resulting in ground tire rubber (GTR). Magnets separate steel wires from the rubber, and both materials are recycled separately. Rubber powder is used to make rubber mats and other rubber-based articles, and can be incorporated in asphalt used for road pavement. Rubber powder can also be added to different materials to improve impact resistance and durability or for noise reduction.<sup>4</sup>

To be commercially viable, the GTR industry must deliver a product that meets quality standards, a task made difficult due to the wide range of tire composition and additives. Intrinsic characteristics of rubbers (no melt point, no solubility) and batch-to-batch and within-batch variations also make quality control of GTR challenging.

Additional Supporting Information may be found in the online version of this article.

© 2015 Wiley Periodicals, Inc.

Thermogravimetric analysis (TGA) is routinely used for compositional analysis and quantification of carbon black and ash content of GTR (ASTM D6370-99 and E1131-08). Crumb size and size distribution are measured by optical microscopy, although the latter is time-consuming and rarely reported. Cross-link density is measured by swelling experiments, although the small crumb size presents an additional challenge.<sup>5</sup> These methods provide partial characterization, but do not always correlate well with observed changes in crumb behavior during use. Determination of the monomer ratio which directly impacts on thermal and mechanical properties of rubbers is performed by pyrolysis-gas chromatography (ASTM D3452), but cannot always distinguish between SBR samples with different monomer contents.<sup>6</sup> The refractive index method (ASTM D5775) proposed for compositional analysis of polymers is not useful for GTR due to the presence of carbon black and due to the impossibility of making a homogeneous film.

It was decided, in this work, to use both standard SBR samples and real GTR samples from a recycling facility. The latter being ill characterized, benchmark values for elemental content and monomer ratio are first obtained using solid-state proton nuclear magnetic resonance (NMR). This technique has previously been used for ground rubber samples,<sup>7–11</sup> but is not amenable to routine quality-control measurements and, as shown in earlier work, can be difficult to implement for GTR because of the presence of magnetic impurities (metal residues).<sup>12</sup> Elemental content benchmark values are more straightforward to obtain, and a combination of readily available techniques (inductively coupled plasma optical emission spectrometry (ICP-OES), atomic absorption spectrometry (AAS), and elemental (CHNS) analysis) is used to provide a thorough characterization of samples, although these suffer from time-consuming sample preparation and are not ideal in the context of industrial rubber recycling quality control.

TGA has been suggested as a means to obtain information on the butadiene/styrene (*B/S*) ratio of SBR. Shield and Ghebremeskel<sup>13</sup> showed that SBR content is related to shifts of the thermal degradation peaks, but these shifts can also be affected by the distribution of styrene in the copolymers (random or block) and by the diene microstructure. Castaldi and Kwon<sup>14</sup> performed TGA in air atmosphere and found an interesting phenomenon for neat SBR: a two-stage combustion was attributed to different oxidation rates of the butadiene backbone and styrene aromatic rings. This technique was, therefore, selected for further evaluation in the context of industrial quality control.

For elemental analysis, X-ray fluorescence (XRF) spectroscopy has recently been used to analyze various polymers. Fink *et al.*<sup>15</sup> and Mans *et al.*<sup>16</sup> investigated thermoplastics recycled from electronics enclosures (acrylonitrile butadiene styrene, polystyrene, styrene-butadiene, polyphenylene oxide, and polyvinyl chloride) with this method, whereas Miskolczi *et al.*<sup>17</sup> proposed its use for inorganic compositional analysis in compressed crumb rubber samples. Tertian and Claisse,<sup>18</sup> on the other hand, proposed a sample preparation method based on compression with a cellulose binder, resulting in self-standing disks that can be kept as standard samples for further use. This method was also selected for further evaluation.

This article, therefore, focuses on GTR characterization in terms of metal and atomic content by XRF spectroscopy and monomer composition by TGA and differential scanning calorimetry (DSC).<sup>19–21</sup> Analyses reported include two types of samples. First, standard SBR samples of known composition were prepared in our laboratory and used to ascertain the potential and precision of each technique. Second, five tire sole GTR samples were obtained from a recycling facility and analyzed to provide samples more relevant to the real challenges faced in this field, and to determine to what extent the presence of numerous additives and heterogeneity from various types of tires affect characterization.

## EXPERIMENTAL

### Commercial GTR Samples GTR-A to GTR-E

Commercial SBR samples were provided by Recyclage Granutech Inc. (Plessisville, QC, Canada). Samples were collected randomly from five different batches, designated by the abbreviations GTR-A to GTR-E. Selected samples all having an average particle size of  $500 \pm 10 \mu\text{m}$  were used. Cross-link density and particle size distributions were reported in a previous article.<sup>5</sup> Prior to measurements, all GTR samples were submitted to acetone extraction to remove low-molecular-weight molecules, such as processing oils or organic additives.

### Preparation of SBR Standard Rubber Samples (9CD to 40CD, 0CB to 100CB, and 50CB+G)

In a 100-mL beaker with a magnetic bar, 2 g of a SBR prepolymer (PLF1502, containing a *B/S* monomer weight ratio of 76/24, kindly supplied by the Goodyear Tire & Rubber Co.) was dissolved in 20 mL toluene, heated to 60°C to facilitate dissolution, and stirred until fully dissolved. In a 50-mL Erlenmeyer flask were introduced 10 mg tetramethylthiuram disulfide, 40 mg stearic acid dissolved in 1 mL toluene, and 100 mg ZnO. This accelerator solution was heated at 50°C until complete dissolution was achieved, and was then added to the SBR solution, after which active carbon black (CC N991, Cancarb Limited Inc., Canada) was added (from 0.60 to 1.40 g, corresponding to 30–70 parts per hundred of rubber or phr). Finally, an aliquot of the cross-linking agent corresponding to 0.05–2 phr of a 1.0 mL  $\text{S}_2\text{Cl}_2$  solution in 10 mL toluene was added using a syringe. Carbon black (1.00 g) was added last, while stirring. The resulting mixture was poured rapidly into stainless steel molds previously sprayed with PEI 35838 ORAPI Northern-Cape silicon releasing agent ( $15 \times 15 \text{ cm}^2$  plates having four 0.2 cm deep, 4 cm wide depressions). Solutions were allowed to dry in the molds for around 2 h at room temperature in a hood. Once dry, films were removed from the mold, which was cleaned using ethyl acetate. Mold surfaces were then treated with the silicon releasing agent, and rubber samples were reinserted in the mold, covered with a silicon-treated plate, and placed for 30 min in a Carver press preheated to 180°C.

Exact quantities of each component used during standard sample preparation are reported in Table I–III, along with the abbreviations used in this work. Two types of standard samples were prepared to evaluate the effect of different compositional changes. The first series is composed of standard samples containing 50% carbon black and having the same *B/S* monomer

**Table I.** Amounts Used for Standard SBR Sample Preparation: Proportions of All Components

Component	Mass used (g)	Composition (phr)
SBR	2	100
Stearic acid	0.04	2
TMTD	0.01	0.5
ZnO	0.1	5
S <sub>2</sub> Cl <sub>2</sub>	0.04–0.2	2–10
Carbon black	0.00–1.4	0–70
Milled glass fibers	0.00 and 0.55	0 and 28

ratio, but having varying cross-link densities. These are abbreviated YCD, where CD stands for cross-link density and Y is the numerical value of the sample cross-link density ( $\rho$ ). A series of samples with varying proportions of carbon black was also prepared, with as constant as possible cross-link densities. These are abbreviated ZCB, where CB refers to the presence of carbon black and Z to the amount (w/w %) added to the sample with respect to SBR. In one of these samples, 50CB+G, “+G” indicates the addition of milled glass fibers (731ED, fiber diameter 10  $\mu\text{m}$ , Owens Corning, Toledo, OH). This sample was added to investigate the effect of silica on various rubber measurements (glass transition, thermal resistance, NMR spectra, etc.), as preliminary observations showed the presence of silica in GTR. This is consistent with Michelin’s proprietary silica blends used in tires to lower rolling resistance.

#### Cross-Link Density Measurements

Cross-link density ( $\rho$ ) of the rubber standards was measured by using ASTM D3616 swelling method, slightly modified to take into account sample size. For standard rubbers, samples (1 mm  $\times$  5 mm) were cut from rubber films, weighed accurately, and submerged in toluene. These were allowed to swell for 72 h at room temperature, protected from light. After 72 h, excess solvent was removed using a pipette without touching the swollen gel pieces. Each gel piece was then lightly dabbed with absorbent paper and immediately weighed accurately. For commercial GTR samples, measurements were performed using a modified version of ASTM D6814 as described by Macsiniuc *et al.*<sup>5</sup>

#### Atomic Absorption Spectrometry

Around 50 mg of each sample was placed in a porcelain crucible and calcined at 650°C for 2 h in a muffle oven, after which the temperature was raised to 700°C and held overnight. Residues were quantitatively transferred to a plastic volumetric vial and dissolved in 1 mL hydrofluoric acid. Deionized water (high performance liquid chromatography grade, Milli-Q) was added to bring the volume to 50 mL. Standard solutions of 5–100 ppm were prepared by dilution from an assurance grade standard silicon solution (10,000 mg/L in H<sub>2</sub>O/4.0% F<sup>-</sup> purchased from Spex CertiPrep, Metuchen, NJ). A Perkin Elmer 3110 atomic absorption spectrometer was used with a nitrous oxide (35 mL/min)-acetylene (43 mL/min) flame at the 251.6 nm spectral line position, optimized according to the manufacturer’s recommendations.

#### Inductively Coupled Plasma Optical Emission Spectrometry

ICP-OES (Optima 3000, Perkin Elmer) was performed using a radio frequency power of 1300 W, and gas flows of 15 L/min for plasma, 0.5 L/min for the auxiliary gas, 0.8 L/min for the nebulizer, and 1.5 mL/min for the mobile phase. Sample calcination was performed as reported for AAS. Solutions were prepared by adding deionized water (high performance liquid chromatography grade, Milli-Q) and 10 mL nitric acid (ACS grade, Caledon Laboratories, Georgetown, ON) to solubilize the resulting solid to a final volume of 100 mL.

#### CHNS Elemental Analysis

CHNS elemental analysis was performed on an organic elemental analyzer (Flash 2000, Thermo Scientific, Waltham, MA). Cystine, used as a standard sample, was put in a universal soft tin container (100pc, outside diameter = 5 mm, height = 8 mm, and volume = 157  $\mu\text{L}$ ), which also served as a blank sample. Around 0.5 mg of each sample was encapsulated in the same type of container.

#### Differential Scanning Calorimetry

DSC was performed using a DSC823e (Mettler Toledo) apparatus with a liquid nitrogen cooling accessory. Approximately, 15 mg of sample was encapsulated in an aluminum pan, and DSC measurements were performed by heating from  $-100^\circ\text{C}$  to  $100^\circ\text{C}$  at  $20^\circ\text{C}/\text{min}$  under nitrogen atmosphere, holding the sample at this temperature for 5 min and then cooling back to  $-100^\circ\text{C}$  at  $20^\circ\text{C}/\text{min}$ . A second heating scan was then performed under the same conditions, and is the one reported in all cases.

#### Solid-State <sup>1</sup>H NMR

Solid-state <sup>1</sup>H NMR spectra of SBR samples were recorded on a 400 MHz solid-state NMR spectrometer (Bruker Biospin, Billerica, MA). Standard samples were cut into small pieces prior to introduction in sample tubes, whereas GTR samples were used as such. Each sample was packed in a 4 mm tube and spun at 8 kHz at the magic angle, with scan time varying from 60 to 240 s.

#### Thermogravimetric Analysis

TGA was performed using a TGA/SDTA 851e (Mettler Toledo) apparatus. Between 1 and 2 mg of sample was put in a ceramic pan, and measurements were performed by heating from  $50^\circ\text{C}$  to  $900^\circ\text{C}$  at  $20^\circ\text{C}/\text{min}$  under air atmosphere.

**Table II.** Amounts Used for Standard SBR Sample Preparation: Amount of Cross-link Agent S<sub>2</sub>Cl<sub>2</sub> and Final Measured Cross-link Density for Samples with Constant Carbon Black Content but Varying Cross-link Density (YCD)

Samples	Mass of S <sub>2</sub> Cl <sub>2</sub> (g)	Cross-link density (mol/cm <sup>3</sup> )
9CD	0.04	8.5
11CD	0.08	11.2
25CD	0.12	25.0
29CD	0.16	29.4
40CD	0.20	39.9

**Table III.** Amounts Used for Standard SBR Sample Preparation: Carbon Black and Milled Glass Fiber Amounts Used in the Preparation of Samples with Constant Cross-link Density, within Experimental Error, But Varying Carbon Black Content (YCB)

Sample	Mass of carbon black (g)	Mass of milled glass fibers (g)	Carbon black (phr)	Milled glass fiber (phr)	Carbon black (%)	Milled glass fiber (%)
OCB	0	-	0	-	0	-
3OCB	0.60	-	30	-	22	-
5OCB	1	-	50	-	32	-
6OCB	1.2	-	60	-	36	-
7OCB	1.4	-	70	-	40	-
10OCB	-	-	-	-	100	-
5OCB+G	1	0.55	50	28	27	15

### Energy-Dispersive XRF Spectrometry

Energy-dispersive XRF spectroscopy was performed using a Minipal 4 benchtop XRF spectrometer (PAN Analytical) apparatus equipped with a rhodium anode tube, five tube filters, a helium purge capability, and a silicon drift detector, running at a maximum of 30 kV and 1 mA. The calibration curve was obtained by measuring disks prepared using different quantities of sample GTR-A, dispersed in 0.5 g of cellulose, with the final Zn concentration varying from 20 to 70 w/w %. The additional four GTR samples (GTR-B to GTR-E) were also dispersed in 0.5 g cellulose, to yield samples with concentrations around 30%, 55%, and 64%, which were used to verify whether the method was robust when GTR composition variations occur. All samples were placed in a Carver Press at 10,000 psi for 30 s to form self-standing disks having a diameter of 3 cm and a thickness of approximately 4.5 mm.

## RESULTS AND DISCUSSION

### Chemical Analysis

Chemical analysis of GTR was carried out by ICP-OES, AAS, and CHNS elemental analysis.

One of the first measurements undertaken in this work aimed at determining benchmark atomic composition for randomly selected industrial GTR samples, as these are then used to validate the methods used and to identify specific problems related to the presence of additives or to their granulometry. For this purpose, chemical analysis was performed using ICP-OES, AAS, and CHNS elemental analysis. ICP-OES and AAS are useful to quantify metals and silica present, whereas CHNS analysis is used to determine the amount of sulfur. Results are reported in Table IV.

ICP-OES results show that the most abundant metal found in GTR samples is zinc, with concentrations varying from 1.97 to 2.23 w/w %. This is consistent with the use of ZnO as a catalyst/accelerator.<sup>22</sup> No correlation was found between Zn content and cross-link density, unfortunately but predictably, because ZnO is used as an accelerator and is not part of the cross-links themselves.

Iron is also found in small quantities, which is attributed to the presence of residues from the steel wires removed in the recycling facility. Sodium and calcium are also present in small quantities: these are added as salts such as Na<sub>2</sub>P<sub>2</sub>O<sub>7</sub> and CaCO<sub>3</sub>

during tire fabrication. Other metals are not present above the detection limit of the method.

AAS is used to measure silicon, as silica is often incorporated in tires to decrease rolling resistance. A small, almost constant percentage of silicon (from 0.72 to 0.85 w/w % of SiO<sub>2</sub>) is present. CHNS analysis is finally used to determine the amount of sulfur, which is present in concentrations ranging from 1.2 to 1.7 w/w %. Sulfur forms cross-linking bonds created during vulcanization, and so, the possibility of gaining information on cross-link density from sulfur content was attractive. In a similar study,<sup>12</sup> no correlation was found between cross-link density and sulfur content in EPDM-based GTR. Likewise, it is not possible to quantitatively correlate cross-link density to the quantity of sulfur present in GTR samples in this work, which may stem from the existence of more than one sulfur sources in the samples, as sulfur can also be present in carbon black. Another possible explanation is that individual cross-links are known to contain varying numbers of successive sulfur. The quantity of sulfur found was found to be relatively constant between 1.2 and 1.7 w/w %. The observed sulfur concentration is in agreement with results of Amari *et al.*<sup>23</sup> who reported that typical SBR scrap tires were composed of 1.1% of sulfur. The sample having the highest cross-link density was the one with the lowest sulfur content, whereas if the sole source of sulfur was cross-links, and if the same number of sulfur atoms was found in each cross-link, this sample would have the lowest cross-link density. To compare with TGA results which are presented in the following section, Table IV also includes the sum of calcium, iron, zinc, and silicon expressed as their oxide forms (CaCO<sub>3</sub>, Fe<sub>2</sub>O<sub>3</sub>, ZnO, and SiO<sub>2</sub>).

### Energy-Dispersive XRF Spectrometry

XRF spectroscopy can be used for elemental analysis of elements with atomic number above 11. As it can be performed on solid samples, this technique is highly attractive for both qualitative and quantitative measurements in the industry, and it is used intensively by the mining industry instead of inductively coupled plasma mass spectrometry or AAS, which require labor-intensive and time-consuming sample digestion. XRF spectroscopy has been proposed as a fast and nondestructive tool to quantify rubber and GTR,<sup>15,17,18,25,26</sup> but its use is not widespread, which may, in part, be related to variations caused by granulometry and sample surface in this technique. It has

**Table IV.** Concentration (w/w %) of Metals in GTR as Determined by ICP-OES, of Si (Expressed as SiO<sub>2</sub>) by Aas and of S by CHNS Analysis

	Standard dev.	Detection Limit	GTR-A	GTR-B	GTR-C	GTR-D	GTR-E	Literature values
Residual mass <sup>a</sup>	1	-	8	7	6	8	5	-
Residual mass <sup>b</sup>	3	-	7	9	4	5	3	-
Al	0.02	0.04	0.00	0.00	0.00	0.00	0.00	0.21 <sup>24</sup>
Ca	0.07	0.02	0.17	0.17	0.30	0.19	0.19	0.1 <sup>24</sup>
Cd	-	0.01	0.00	0.00	0.00	0.00	0.00	-
Cr	-	0.01	0.00	0.00	0.00	0.00	0.00	-
Cu	-	0.01	0.00	0.00	0.00	0.00	0.00	-
Fe	-	0.01	0.16	0.30	0.05	0.25	0.00	0.28 <sup>24</sup>
Mg	-	0.01	0.00	0.00	0.00	0.00	0.00	0.84 <sup>24</sup>
Mn	-	0.01	0.00	0.00	0.00	0.00	0.00	-
Na	-	0.01	0.22	0.25	0.05	0.22	0.05	-
Ni	-	0.01	0.00	0.00	0.00	0.00	0.00	-
Zn	0.2	0.04	2.2	2.0	2.0	2.0	2.2	1.5 <sup>23</sup>
CaCO <sub>3</sub> , ZnO, Fe <sub>2</sub> O <sub>3</sub> , SiO <sub>2</sub>	0.02	-	4.15	4.12	4.10	4.09	4.08	-
SiO <sub>2</sub>	0.02	0.03	0.72	0.79	0.78	0.80	0.85	0.6 <sup>24</sup>
S	0.1	0.001	1.2	1.7	1.3	1.6	1.5	1.1 <sup>23</sup>

<sup>a</sup>As determined from calcinations prior to spectrometry measurements.

<sup>b</sup>As determined from TGA analysis (see later section).

been used on vulcanized styrene copolymers,<sup>27</sup> recycled thermoplastics from electronic waste,<sup>15</sup> as well as waste GTR.<sup>17</sup> The latter study showed very interesting results, with differences between XRF spectroscopy and ICP-OES below 8%. It was, therefore, decided to investigate this technique in this work to verify whether the results would be as good with different GTR sources.

Samples for XRF analysis were initially prepared as proposed by Miskolczi *et al.*<sup>17</sup> by hand pressing of the GTR powders. Initial trials with this technique resulted in brittle samples which could not be kept easily for further measurements or as control samples, and standard deviations were found to be very high. This was attributed to poor compactness and high heterogeneity, due to the granulometry of GTR. The use of a cellulose binder was tested next, following the work of Tertian and Claisse<sup>18</sup> on powdered samples. This method also allows disk conservation for subsequent recalibration, which is useful for quality control. Standard SBR films were grinded and used to establish a calibration curve, but results were inconsistent with those of GTR samples because of differences in powder granulometry, morphology, and composition. Instead, a single GTR sample selected at random (GTR-A) was used to build a calibration curve by varying the mass of GTR used to form the disks.

A typical qualitative fluorescence diagram of such a sample, using GTR-A, is given in Figure 1, where it is compared with the spectrum of neat GTR (held in a sample cup with a polyethylene terephthalate film bottom). Dilution decreases peak intensity by a factor of approximately 2, but each of the

observable peaks remains clear and well defined. The most intense peaks correspond to zinc, iron, and, to a lesser extent, bromine. Only the zinc peak presents an intensity large enough for quantitative analysis.

Figure 2 reports the calibration curve of the Zn K $\alpha$  peak intensity as a function of Zn content (determined by ICP-OES) in cellulose-based disk specimens prepared by varying the quantity of GTR. The measurable upper concentration is limited by the quantity of GTR that can be included in a disk. A maximum of 70 w/w % GTR can be placed in a disk, which results in a linearity limit of 1.6 w/w % in the GTR powder. Higher Zn content in a disk leads to elastic specimens, which are difficult to press into firm, self-standing. The calibration curve shows a good linear relationship between intensity and Zn content, especially considering the inherent inhomogeneity of GTR samples. Limit of detection and of quantification are 0.8 and 1.1 w/w % Zn in a GTR sample, respectively.

It must be noted that, in Figure 2, the disk concentration is used, and not the concentration in the initial GTR sample, as varying quantities of GTR-A were used to achieve this calibration curve. The use of this calibration curve must, therefore, be followed by a correction for the dilution factor.

The disk concentration obtained from the calibration curve, Z<sub>N-DISK</sub>, is first transformed into concentration in the GTR sample, Z<sub>N-XRF</sub>. This operation is straightforward, following:

$$Z_{N-XRF} = Z_{N-DISK} \times (m_{GTR} + m_{cellulose}) / m_{GTR} \quad (1)$$

where  $m_{GTR}$  and  $m_{cellulose}$  are the masses of the GTR sample and cellulose in the disk, respectively.

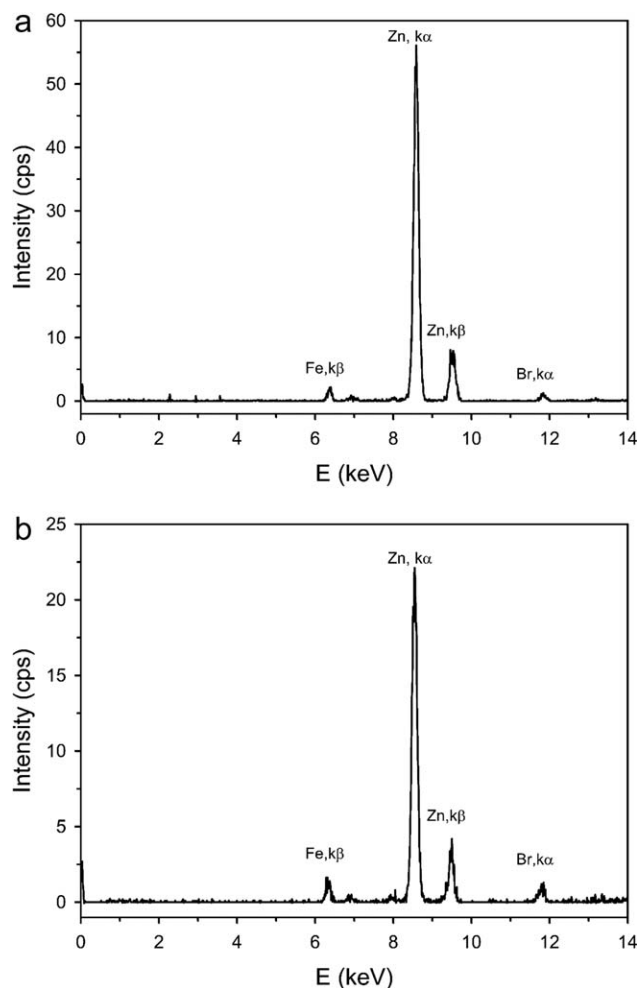


**Figure 1.** X-ray fluorescence spectra for a representative GTR sample (GTR-A). (a) GTR-A sample without binder. (b) GTR-A disk with cellulose binder (55 w/w % GTR).

To verify whether a curve obtained with a single standard sample can be used to determine correctly the zinc content of GTR samples having different compositions, GTR-B to GTR-E were then measured using three different GTR disk concentrations, and resulting measurements are presented in Figure 2. These data points generally lie close to the calibration curve, although they are not distributed randomly but tend to lie above the curve, indicating a possible systematic error, which is, however, in the range of the estimated standard deviation.

Table V reports Zn concentrations calculated from the calibration curve in Figure 2 ( $Zn_{XRF}$ ) and compares these with the values obtained from ICP-OES. Detailed ICP-OES and XRF spectroscopy data are reported in Supporting Information. In all cases, the error is smaller than the error estimated with a 95% probability using Student's *t*-test. Relative errors obtained when compared with  $Zn_{ICP}$  ICP-OES measurements vary from 4% to 14%, which shows that both methods are in good agreement.

The correlation observed in Figure 2, combined with the good fit of GTR samples using their ICP-OES determined zinc

percentages, confirms that the use of a single standard to build the calibration curve is effective in eliminating matrix effects and allows determination of zinc content with absolute values.

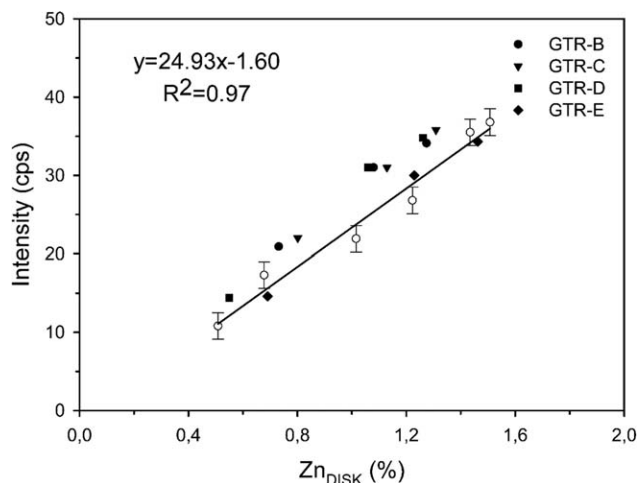
It is concluded that XRF spectrometry is a nondestructive, fast, and affordable technique for elemental determination of Zn in SBR-based GTR samples. Although this method shows a lower precision and higher detection limit than ICP-OES, because of its low maintenance, low cost, and low time requirement for sample preparation, it is a very attractive method for quality control in the industry.

The next aspect that will be discussed is the relative proportion of styrene and butadiene, as well as the possible presence of other polymers in the GTR samples. This will be investigated using NMR, TGA, and DSC in the following sections.

#### Solid-State NMR Investigation of Monomer Ratio

Solid-state NMR spectroscopy is extremely powerful to investigate the chemical structure of insoluble material, but unfortunately, because of the high cost of the instrument and of its maintenance, solid-state NMR is not easily available to recycling facilities. Nevertheless, in this work, it has been used to further characterize the samples. For standard SBR samples of known (*B/S*) monomer ratio, this will provide a confirmation that NMR-determined values are quantitative in the conditions used, whereas for industrial GTR samples of unknown composition, this will provide benchmark values of allylic (mainly butadiene from SBR and isoprene) versus aromatic (styrene), (*B + I/S*, monomer ratios, as isoprene from natural rubber is also found in these samples.

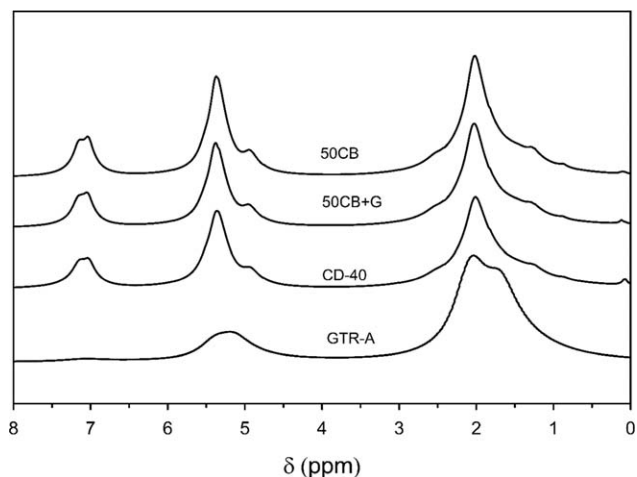
Figure 3 reports NMR spectra of representative samples studied in this work. GTR samples have much higher peak width than SBR standard samples, which is attributed to the presence of residual paramagnetic iron in GTR samples,<sup>12</sup> causing an increase in  $T_2$ .<sup>9</sup> Because of this peak broadening, it is not possible to ascertain the relative proportions of different microstructural features for GTR samples. Three main peak regions can be seen in the spectra: a peak centered around 7.0 ppm, attributed



**Figure 2.** Calibration curve of Zn using XRF (GTR-A contents in cellulose disk samples between 20 and 70 w/w %) as a function of Zn concentration in the disk.

**Table V.** Zn Concentration as Determined from the XRF Calibration Curve and Compared with ICP-OES Results for GTR-B to GTR-E

GTR sample	Experimental XRF data		Zinc percentages as calculated by XRF						Comparison with ICP-OES results		
	mw (g)	mc (g)	I (cps)	Zn in disk (w/w %)	Zn in GTR (w/w %)	Average Zn in GTR (w/w %)	Standard deviation (w/w %)	Error with 95% confidence (± %)	Zn <sub>ICP</sub> (%)	Zn <sub>ICP</sub> -Zn <sub>XRF</sub> (w/w %)	Relative error (%)
GTR-B	0.2957	0.5088	20.9	0.77	2.11	2.10	0.07	0.18	1.99	0.11	5
	0.6015	0.5070	31.0	1.18	2.17						
GTR-C	0.8985	0.5045	34.1	1.30	2.04				2.04	0.08	4
	0.3234	0.4998	22.0	0.82	2.08	2.12	0.03	0.08			
GTR-D	0.6248	0.5040	31.0	1.18	2.13				1.97	0.07	4
	0.9073	0.5070	35.8	1.37	2.14						
GTR-E	0.2115	0.5465	14.4	0.51	1.84	2.04	0.18	0.45	2.19	0.31	14
	0.5861	0.5035	31.0	1.18	2.19						
GTR-E	0.8962	0.5038	34.8	1.33	2.08						
	0.2454	0.5325	14.6	0.52	1.65	1.88	0.20	0.5			
GTR-E	0.6547	0.5117	30.0	1.14	2.03						
	1.0245	0.5090	34.3	1.31	1.96						

**Figure 3.** Solid-state  $^1\text{H}$  NMR spectra of representative samples.

to styrene aromatic ring protons, peaks between 5.0 to 5.2 ppm attributed to hydrogen atoms on butadiene double bonds that have not been opened by the vulcanization process, and finally, around 1.5–2.5 ppm, peaks associated to methyl and methylene groups. The main difference that can be noted between standard SBR and GTR spectra is the very low intensity of the styrene peak at 7.0 ppm for GTR samples (an enlargement of this peak region can be found in Supporting Information Figure A2). This small intensity is in agreement with the use, in rubber tire soles, of a mixture of SBR and natural rubber, thus decreasing the styrene content. This, combined to peak broadening, results in the low intensity of the 7 ppm styrene peak for GTR samples.

In the 5 ppm region, two main peaks are observed: the main intensity peak at 5.2 ppm, which corresponds to  $-\text{CH}=\text{CH}-$  protons of 1,4 butadiene segments, and a much smaller peak around 4.9 ppm, which is attributed to  $\text{CH}_2=\text{C}-$  groups.<sup>28</sup> The relative intensity of this peak is much smaller as compared with the peaks in the 1–2 ppm region, indicating a lower quantity of double bonds, related to a smaller quantity of SBR due to blending with natural rubber and possibly other aliphatic rubbers.

Aliphatic protons are observed in the last region of NMR spectra. For SBR, the highest peak is observed at 2.1 ppm, attributed to aliphatic  $\text{CH}_2$  groups, although smaller peaks appear from 0.9 to 2.7 ppm, corresponding to microstructural variations. On the other hand, in GTR samples, two peaks of similar intensities are clearly present at 1.8 and 2.1 ppm, assigned, respectively, to  $\text{CH}_3$  and  $\text{CH}_2$  aliphatic groups. Whereas  $\text{CH}_2$  group can be associated to the presence of styrene, butadiene, or other aliphatic rubbers, the peak at 1.8 ppm, attributed to methyl groups, is in agreement with the presence of an important amount of polyisoprene, of which natural rubber is composed. Relative intensities are similar to that observed in natural rubber, although the  $\text{CH}_2$  peak is more prominent, as expected from the presence of SBR.<sup>29,30</sup>

Relative NMR peak intensities were used to ascertain the relative proportion of styrene. To do this, it was supposed that all

**Table VI.** Monomer Weight Ratio ((*B* + *I*)/*S*) from NMR Data and SBR Manufacturer *B*/*S* Value

Sample	( <i>B</i> + <i>I</i> )/ <i>S</i> NMR	<i>B</i> / <i>S</i> data from manufacturer	Cross-link density ( $\times 10^{-5}$ mol/cm <sup>3</sup> ) $\pm 1$
GTR-A	99/1 $\pm 3$	-	96
GTR-B	98/2 $\pm 3$	-	13
GTR-C	95/5 $\pm 3$	-	10
GTR-D	94/6 $\pm 3$	-	9
GTR-E	94/6 $\pm 3$	-	8
OCB	78/22 $\pm 2$	76/24	13
3OCB	74/26 $\pm 2$	76/24	16
5OCB	77/23 $\pm 2$	76/24	25
6OCB	78/22 $\pm 2$	76/24	20
7OCB	77/23 $\pm 2$	76/24	23
5OCB+G	77/23 $\pm 2$	76/24	16

polymers are composed of styrene and aliphatic rubbers (mainly butadiene and isoprene). The monomer ratio is calculated as:

$$\frac{(B+I)}{S} = \frac{5(I_5 + (I_2 - 3I_7/5))}{6I_7} \quad (2)$$

where  $I_5$  the intensity of the peak at 5.0–5.2 ppm, corresponding to CH allyl hydrogen atoms of aliphatic rubbers;  $I_2$  the intensity of the peaks between 1 and 3 ppm and centered around 2 ppm, which correspond to  $\text{CH}_3$ ,  $\text{CH}_2$ , and CH groups of all rubbers present, and from which the styrene aliphatic proton are removed using the  $3I_7/5$  term;  $I_7$  is the intensity of the peak at 7 ppm, attributed to aromatic styrene protons. The  $5/6$  term is used to take into account the number of protons of each chemical group (5 for styrene and 6 for butadiene), which supposes that butadiene represents the largest proportion of aliphatic rubbers in the GTR samples and that it is only composed of 1,4 units. This evaluation is, therefore, semi-quantitative, and includes the following approximations:

1. Allylic protons that are transformed into aliphatic protons upon cross-linking are negligible as compared with those remaining,
2. Butadiene is composed only of 1,4 linkages, a reasonable approximation for SBR prepared by emulsion polymerization, which is known to contain less 1,2-linked units than solution SBR obtained by anionic polymerization,
3. Butadiene and isoprene both have the same number of protons per chemical unit and the same distribution of allylic and aliphatic protons.

Results are reported in Table VI, and although this approach is semi-quantitative, a good fit is observed between the *B*/*S* weight ratio supplied by the manufacturer for the initial non-cross-linked SBR matrix (76/24) and the (*B* + *I*)/*S* value determined by NMR for the standard SBR samples, which is equivalent to *B*/*S* in the absence of isoprene in these samples, and which varies from 78/22 to 74/26, with an observed standard deviation of 2%.

Proportions of aliphatic rubber and styrene (*B* + *I*)/*S* in GTR samples are also reported in Table VI, and these show values of

94/6 to 99/1, with a standard deviation of 3%. Calculations were also performed using a different approximation, by supposing that all aliphatic and allylic protons belonged to isoprene units instead of butadiene units, with little effect on the resulting percentages, because of the low intensity of the aromatic proton peak of styrene. The observed values correspond to the presence of only 2 w/w % styrene. This is lower than percentages found in pure SBR, which normally vary from 10 to 40 w/w % styrene, as expected because tire sole are composed of blends of SBR, natural rubber, and polybutadiene.<sup>31</sup> Further, as discussed earlier, NMR results show that large amounts of polyisoprene are present. Polybutadiene, when present, will further decrease the (*B* + *I*)/*S* ratio, and the quantity present could not be determined in this case because of the above-mentioned peak broadening.

Surprisingly, although samples were taken in five different lots, all GTR samples show the same (*B* + *I*)/*S* ratio, within the standard deviation of the method. NMR is, therefore, not precise enough, in this case, to study changes in (*B* + *I*)/*S* ratio between these samples. More importantly, as all industrial samples showed similar values of (*B* + *I*)/*S* ratio, this indicates that monomer ratio may not be a critical parameter for GTR within a given recycling facility, depending on the tire source used. Nevertheless, using the NMR-determined benchmark (*B* + *I*)/*S* ratios, the possibility of using TGA for both carbon black and *B*/*S* or (*B* + *I*)/*S* ratio determination will be discussed next, as combining both characterizations in a single step could decrease the time needed for quality control.

#### Thermogravimetric Analysis

TGA is used for routine carbon black and fillers (inorganics) present in rubbers, as described in ASTM D6370-99 and E1131-08. It has also been proposed for semi-quantitative estimation of cross-link density in EPDM GTR samples in a previous article.<sup>12</sup> Furthermore, as discussed in the Introduction section, Castaldi and Kwon<sup>14</sup> have previously observed a two-stage combustion attributed to different oxidation rates of butadiene and styrene in SBR. It was, therefore, decided to verify in this work



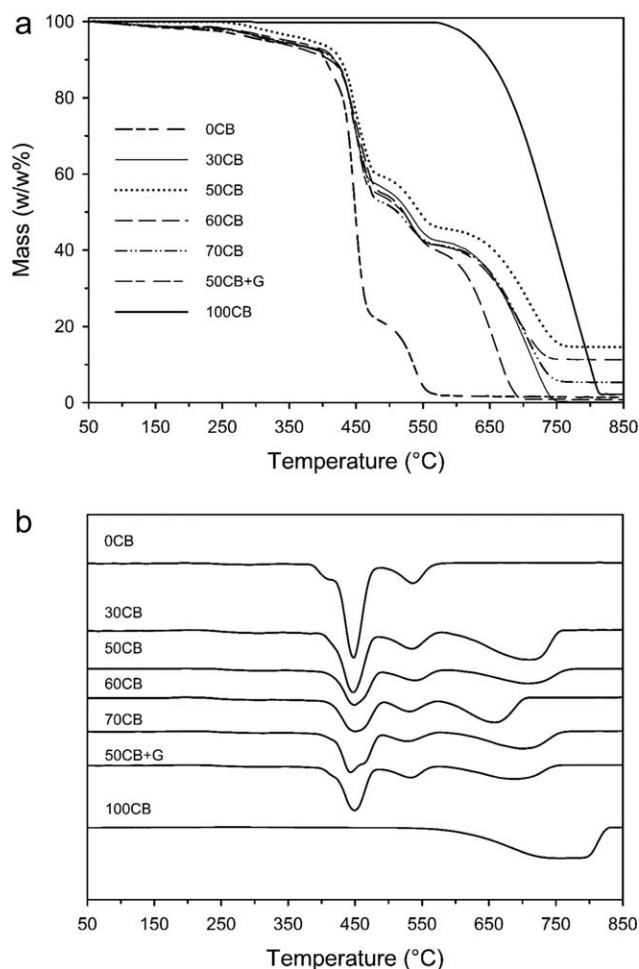


**Figure 4.** TGA of standard SBR samples with different carbon black contents. (a) Degradation scans. (b) First derivatives of a typical scan.

whether this phenomenon could be used to investigate, quantitatively or semi-quantitatively, the monomer ratio in GTR samples.

In this work, a series of SBR standard samples with varying proportions of carbon black and similar cross-link densities was prepared and investigated using TGA under air atmosphere. The corresponding degradation curves are shown in Figure 4(a). The decomposition process is clearly divided into three stages, which start at 350°C, 450°C, and 550°C, respectively. The number of degradation steps is different from that observed for EPDM samples discussed in a previous article,<sup>12</sup> for which two main degradation steps are observed: a first step at 400°C, corresponding to the degradation of the rubber organic phase, and a second step, at 550°C, corresponding to the oxidation of carbon residues formed in the first step, as well as carbon black initially present in samples, to carbon dioxide. Sulfur present in cross-links has previously been shown to degrade near 400°C, whereas sulfur present in carbon black degrades at higher temperatures (around 550°C), both yielding SO<sub>2</sub>.<sup>12</sup>

The occurrence of an additional weight loss step is normally associated with multiple mechanisms that are dominant at

certain temperatures or reaction times.<sup>32</sup> This is typically observed for samples containing more than one type of compound, or when an important difference in thermal resistance exists between some of the compounds. In SBR, the first degradation step around 350°C–440°C is attributed to butadiene units and possibly to aliphatic carbon atoms of styrene units. The second step, between 450°C and 540°C, is associated to the combustion of the remaining styrene benzene rings, which require a higher activation energy to oxidize.<sup>14</sup> The third step, starting around 550°C, is similar for most rubbers and organic materials, and is related, as in the case of EPDM-based waste ground rubber, to the combustion of carbon to form carbon dioxide.<sup>21,33</sup> As reported in Figure 4(a), degradation of the standard SBR samples containing no carbon black (sample 0CB) is mostly complete upon reaching a temperature of 600°C, and the third degradation step can be used to determine directly the quantity of carbon black in the initial samples. Calculating the first derivatives, shown in Figure 4(b), allows a straightforward and unambiguous evaluation of degradation temperatures in each step.

Above 750°C, the curves do not reach zero because of remaining minerals such as ZnO. This residual mass is often designated as the ash content, or residual minerals. Mass percentages corresponding to the sum of the two first peaks for SBR, the second peak for carbon black, and the last peak for residual minerals are reported in Table VI. These values are used to estimate the amount of carbon black and of residues. It must be noted that the sum of SBR, ZnO, and SiO<sub>2</sub> percentages used to prepare the samples do not total 100% because of the small quantity of stearic acid used, which is not taken into account in the calculation, and to S<sub>2</sub>Cl<sub>2</sub>, part of which evaporates and oxidizes to SO<sub>2</sub> during cross-linking. A good fit is observed, as expected, between the percentage of carbon black used to prepare standard samples and third TGA mass loss. Residual mass percentages also fit, within experimental error, with the quantity of inorganic substances (ZnO and SiO<sub>2</sub>), used to prepare the standard samples, as these do not degrade in temperature range tested. This accounts for 2–5 w/w % of mass loss, with the exception of sample 50CB+G, which contains milled glass, and, therefore, shows a much higher residual percentage of 18 w/w %.

It was attempted to determine the relative composition of styrene and butadiene by using the second peak to account for aromatic rings in styrene thermal degradation, thus allowing calculation of the weight percentage of styrene *S* as:

$$S(\text{w/w}\%) = \frac{2\text{nd mass loss (w/w}\%)}{\left(\frac{77}{104}\right)} \quad (3)$$

where the second mass loss is measured by thermogravimetry between 500°C and 550°C and is mainly attributed to the degradation of styrene units, and 77/104 corresponds to the molar mass ratio of the benzene ring in the styrene repeating unit.

The first peak, related to the degradation of aliphatic groups, is taken as the sum of aliphatic rubbers (butadiene, isoprene, or other aliphatic rubber units) and of the aliphatic backbone of

Table VII. TGA Degradation Temperatures and Relative Mass Loss Percentages for Standard Samples

	Onset Tdegr 1 (°C)	First mass loss <sup>a</sup> (w/w %)	First mass loss <sup>b</sup> (w/w %)	Onset Tdegr 2 (°C)	Second mass loss <sup>a</sup> (w/w %)	Second mass loss <sup>b</sup> (w/w %)	First + Second mass losses <sup>a</sup> (w/w %)	First + Second mass losses <sup>b</sup> (w/w %)	SBR used (w/w %)	Onset Tdegr 3 (°C)	Third mass loss <sup>a</sup> (w/w %)	Third mass loss <sup>b</sup> (w/w %)	Carbon black used (w/w %)	Residual mass (w/w %)	ZnO + glass used (w/w %)
OCB	346	79	80	491	19	18	98	98	95	-	-	-	-	2	5
30CB	348	64	65	509	16	10	80	75	74	601	15	20	22	5	4
50CB	369	52	52	484	13	11	65	63	65	610	31	33	32	4	3
60CB	358	45	46	496	15	11	60	57	61	571	38	41	36	2	3
70CB	362	47	47	489	11	9	58	56	57	576	37	39	40	5	3
50CB+G	358	45	46	492	13	11	58	57	55	594	29	30	27	13	18

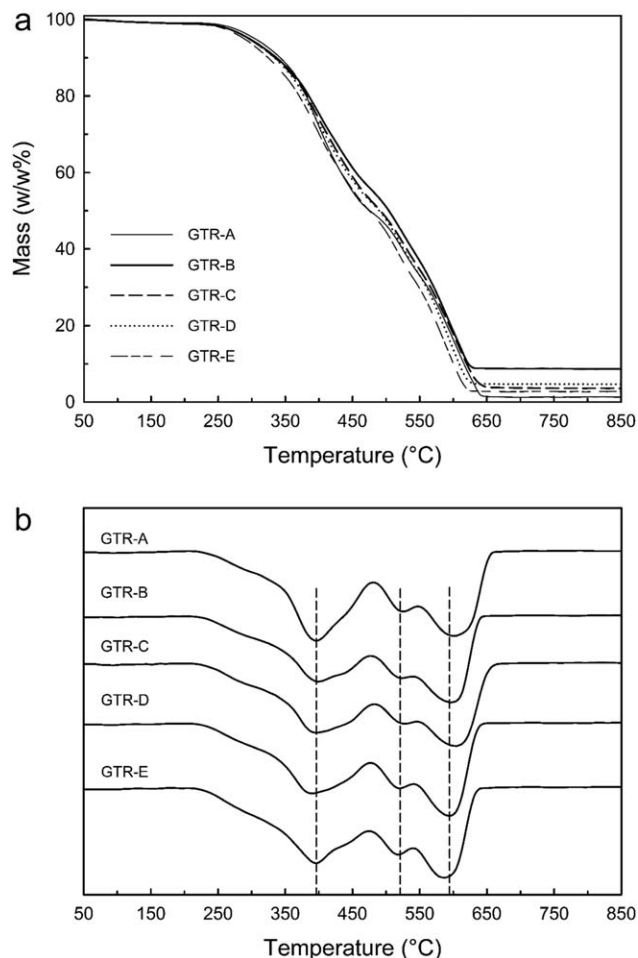
<sup>a</sup> Using temperatures determined by first derivatives.<sup>b</sup> Using fixed temperature ranges of 500°C, 550°C, and 750°C.

Figure 5. TGA temperature scans for GTR samples. (a) Degradation curves. (b) First derivatives.

styrene, and is, therefore, used to approximate the quantity of aliphatic rubbers ( $B+I$ ) w/w % as:

$$(B+I)(w/w\%) = 1st\ mass\ loss\ (w/w\%) - \left( S(w/w\%) \times \left( \frac{27}{104} \right) \right) \quad (4)$$

where 27/104 corresponds to the mass ratio of aliphatic groups in the styrene unit. From these two percentages, the  $(B+I)/S$  weight ratio, which is equal to the  $B/S$  weight ratio for neat SBR, can be calculated and is compared in Table VII with the value supplied by the manufacturer. All samples were prepared with the same prepolymer and, therefore, have the same  $B/S$  ratio. When using fixed temperatures for calculations, a higher  $B/S$  or  $(B+I)/S$  value for SBR standard samples is obtained from TGA as compared with the manufacturer value, indicating that TGA-determined values using fixed temperatures are not quantitative. On the other hand, for TGA values obtained at temperatures defined by the first derivative, values obtained are slightly higher than NMR-determined values, but correspond within two standard deviations to the supplier value, indicating that TGA can be used to quantify, to a precision of 4%, the proportion of butadiene and styrene in the rubber chains of standard SBR samples. It can also be noted that the presence of carbon black does not affect these results.

**Table VIII.** Calculation of Butadiene Percentage in SBR Rubber Molecules for Standard Samples also Containing Carbon Black, and for GTR Samples as Determined by NMR and TGA

Samples	Supplier value (w/w %)	TGA (w/w %)					
		Fixed temperatures (500°C, 550°C, and 750°C)		Positions determined by first derivatives		NMR (w/w %)	
OCB	76	82	83 ± 2 <sup>a</sup>	80	79 ± 2 <sup>a</sup>		78
3OCB	76	82		78		74	
5OCB	76	84		77		77	
6OCB	76	80		76		78	
7OCB	76	86		81		77	
5OCB+G	76	82		79		77	
GTR-A	-	82	81 ± 2 <sup>b</sup>	79	75 ± 3 <sup>b</sup>	99	96 ± 3 <sup>b</sup>
GTR-B	-	83		73		98	
GTR-C	-	80		75		95	
GTR-D	-	79		72		94	
GTR-E	-	79		73		94	

<sup>a</sup> average over all CB samples.<sup>b</sup> average over all GTR samples.

TGA was also performed on the same series of commercial GTR samples for which NMR benchmark ( $B + I$ )/ $S$  values were measured, as reported in Figure 5. GTR samples have first been submitted to a Soxhlet extraction, as it is known that below 350°C a first mass loss appears in the degradation process of many industrial SBR samples, attributed to the volatilization of processing oil, excess curatives, or other organic additives with low boiling-points.<sup>33,34</sup> This first degradation process is, therefore, absent from the TGA scans reported in this study. For GTR samples, the same three degradation steps observed in standard SBR samples are present, but they are not as distinct, which may be due to variations in molecular weight, cross-link density, and composition of tires used to prepare GTR powders. Three degradation steps can, however, be clearly distinguished on the first derivative curve in Figure 5(b). As in the case of standard SBR samples, these curves are used to determine the quantity of carbon black, inorganic residuals, and, tentatively, ( $B + I$ )/ $S$  content. Two methods are used to determine the  $B/S$  ratio: fixed temperature ranges and temperature ranges determined by first derivatives, which are indicated as dashed lines on Figure 4(b).

Quantification of GTR samples is reported in Table VIII. The main difference as compared with standard SBR samples is the higher residual mass, varying from 2.7 to 8.8 w/w %, which fits, within experimental error, with the sum of residues as determined from calcination prior to ICP-EOS and AAS measurements, as reported in Table IV. These residues are mostly composed of ZnO, CaCO<sub>3</sub>, SiO<sub>2</sub>, and iron oxide (mainly Fe<sub>2</sub>O<sub>3</sub>).

As in the case of standard SBR samples, TGA is used to estimate the monomer weight ratio, expressed as ( $B + I$ )/ $S$ , which is reported in Table VIII. For GTR samples, TGA-obtained values are underestimated by 15%–21% for the fixed temperature and first derivative-determined temperatures, respectively, as compared with benchmark NMR-determined values, whereas a standard deviation

of 2%–3% is calculated from measurements performed on three to five different samples of each GTR. The TGA method clearly overestimates the quantity of styrene present. On one point, both methods are in agreement: differences in ( $B + I$ )/ $S$  ratio between the various GTR samples studied are small.

These results clearly show that no quantitative evaluation can be made using TGA in the case of industrial GTR samples. This is attributed to the loss of definition in the TGA degradation pattern as seen in Figures 4 and 5: whereas each degradation step was well defined in standard SBR samples, an almost continuous degradation is observed for GTR, as mentioned earlier in this article. This continuous degradation is related to GTR composition, as an important percentage of natural rubber is present, having a degradation temperature intermediate between those of butadiene and styrene, and, therefore, causing the observed transition widening. Furthermore, the quantity of styrene in GTR samples is close to the detection limit of this technique, thus contributing to make this method unsuitable for GTR samples. TGA determination of SBR content can, therefore, be useful for GTR samples made from SBR not mixed with other rubbers (from sources other than tires), but not from tire recycling sources.

In conclusion, for samples composed of SBR, TGA can be used to determine the content of carbon black and of inorganic additives (as ash content), and can also be used to estimate the monomer  $B/S$  ratio. Unfortunately, because of the limited amount of styrene and the presence of natural rubber, estimations of the ( $B + I$ )/ $S$  monomer ratio cannot be made for GTR samples using TGA. The use of TGA to determine the  $B/S$  ratio of waste ground SBR from other sources is however proposed, as TGA is already used for determination of carbon black and of inorganic residues, and therefore, this may improve quality control measurements without increasing measurement time.

**Table IX.** DSC-Determined  $T_g$  Values and Swelling Measurement Cross-link Density Results for Standard and GTR Samples

Sample	$T_g$			$T_g$ width	Cross-link density ( $\times 10^{-5}$ mol/cm <sup>3</sup> )
	Onset (°C)	Midpoint (°C)	Endpoint (°C)	Endpoint-onset (°C)	
<b>SBR standard samples—carbon black same concentration of sulfur</b>					
OCB	−54	−49	−45	9	12.5
30CB	−55	−50	−46	9	16.1
50CB	−54	−49	−45	9	25.0
60CB	−54	−49	−45	9	20.2
70CB	−54	−50	−46	8	22.5
50CB+G	−53	−48	−44	9	15.7
<b>SBR standard samples—50% carbon black, varying cross-link density</b>					
40CD	−53	−48	−43	10	39.9
29CD	−54	−49	−45	9	29.4
25CD	−54	−49	−45	9	25.0
11CD	−55	−51	−48	7	11.2
9CD	−54	−50	−47	7	8.5
<b>GTR</b>					
GTR-A	−61	−54	−48	13	95.8
GTR-B	−61	−54	−49	12	12.7
GTR-C	−61	−54	−50	11	9.6
GTR-D	−61	−54	−49	12	8.5
GTR-E	−61	−54	−49	12	8.2

### Thermal Analysis by Differential Scanning Calorimetry

Thermal transitions have a direct effect on physical and mechanical properties of polymers, and are easily investigated using DSC. The glass-transition temperature ( $T_g$ ) can be affected by many factors, including crystallinity, cross-link density, efficiency of vulcanization, composition and microstructure, molecular weight, and presence of additives.<sup>35,36</sup> For this reason, standard samples were prepared with controlled cross-link densities and carbon black content, using the same SBR rubber source and, therefore, having the same  $B/S$  monomer ratio.

Table IX reports values for glass-transition temperature  $T_g$  determined for onset, midpoint, and endpoint for standard samples with varying cross-link density (DSC thermograms are available in Supporting Information). All values are very similar, and do not vary by more than the experimental error of 1°C–2°C. Thus, within the cross-link density range used in this work, which corresponds to the range of cross-links found for GTR samples, cross-links do not affect significantly the position of the  $T_g$  transition. For samples with different carbon black contents, likewise, variations are very small, of the order of the experimental error. This indicates that the effect of confinement due to the presence of carbon black, for up to 70 w/w %, on glass-transition temperature  $T_g$  is negligible. It is concluded that changes in the glass-transition temperature of GTR samples would be indicative of a change in GTR monomer composition, although these would be difficult to quantify, because of the rubber microstructure variations.

As compared with  $T_g$  values of standard SBR samples, all GTR samples have a  $T_g$  lower by 5°C. Carbon black and cross-link density cannot account for this difference, which is, therefore, attributed to a difference in  $(B + I)/S$  monomer ratio.<sup>35</sup> This is in agreement with the lower quantity of styrene in GTR, as polystyrene has a higher glass-transition temperature (95°C–128°C) than polybutadiene (−103 to −55°C) or natural rubber (*cis*-polyisoprene, −73°C to −69°C).<sup>37</sup> Because of the complex blend of rubbers in GTR, it is not expected that  $T_g$  could provide a quantitative evaluation of rubber compositions, but any significant change in rubber composition could be detected by comparing  $T_g$  values. All GTR samples have the same  $T_g$  value, within experimental error, in agreement with NMR results that no significant change in  $(B + I)/S$  monomer ratio was noted for the GTR samples studied.

Although  $T_g$  position does not vary from one sample to another,  $T_g$  transition width does. For standard samples, the width varies from 7°C for samples having the lowest cross-link density, to 10°C for that having the highest cross-link density. GTR samples have slightly higher  $T_g$  widths as compared with standard samples, which is attributed to a higher composition heterogeneity. Interestingly, the sample with the highest width, GTR-A, is the one which has the highest cross-link density, thus confirming that the width can provide insights on cross-link density in the range studied. It should, however, not be used for quantification, as too many factors affect  $T_g$ , and as sample inhomogeneity may also lead to  $T_g$  width enlargement.

## CONCLUSIONS

Investigation of the usefulness of XRF spectroscopy, DSC, and TGA for quality control purposes (in addition to the well-established carbon black content determination by TGA) is reported in this article. A thorough investigation of commercial GTR samples and of standard SBR samples was first performed, to provide benchmark values.

XRF spectroscopy was used to quantify zinc in GTR samples. It is found essential to use a real GTR sample to provide a standard curve, because of matrix effects. Compressing the samples into pellets or disks in the presence of cellulose results in good repeatability. This rapid, simple, and straightforward technique is, therefore, recommended in facilities where zinc quantification is an issue.

Thermogravimetry provides reliable semi-quantitative  $B/S$  ratios in neat SBR samples, but overestimates the  $(B + I)/S$  monomer ratio of GTR samples, which is attributed to the small amount of styrene units present and to the presence of other types of rubbers which degrade in temperature ranges intermediate to those of butadiene and styrene rubber units. It is unfortunately not recommended for this purpose in tire recycling facilities, although it can be recommended for recycled parts in which the only rubber present is SBR. Finally, DSC can be recommended as a complementary source of qualitative quality control, as large changes in  $(B + I)/S$  ratio can be identified through variations in the glass-transition temperature.

This work also shows that techniques that are quantitative or semi-quantitative in the case of neat SBR (such as  $B/S$  TGA determination) can be of more limited use for SBR-based GTR. Challenges remain in finding rapid techniques for estimation of the cross-link density, and in improving the quantification of the  $B/S$  ratio.

## ACKNOWLEDGMENTS

The authors acknowledge the financial support of the Natural Sciences and Engineering Research Council of Canada (NSERC). H. Liang benefitted from a scholarship from the Chinese Scholarship Council, and thankfully acknowledges this support. Goodyear Tire & Rubber Co. and Recyclage Granutech Inc. (Plessisville, QC, Canada) are also thanked, respectively, for providing SBR prepolymers and waste ground rubber used in this work. The assistance of R. Plesu (TGA), P. Audet (solid-state NMR), S. Groleau (AAS and ICP-OES), and J.-M. Hardy (standard sample preparation), from the Department of Chemistry, Université Laval, and A. Macciniuc (advice on sample preparation) from the Department of Chemical Engineering, Université Laval, are also gratefully acknowledged.

## REFERENCES

1. Karger-Kocsis, J.; Mészáros, L.; Bárány, T. *J. Mater. Sci.* **2013**, *48*, 1.
2. United States Environmental Protection Agency. Waste-s – Resource Conservation – Common Wastes & Materials – Scrap Tires. Available at: <http://www.epa.gov/osw/conserv/materials/tires/basic.htm>, accessed on January 2014.
3. White, J. R.; De, S. K. *Rubber Technologist's Handbook*; Rapra Technology Limited: Shawbury, **2001**; p 131.
4. Fang, Y.; Zhan, M.; Wang, Y. *Mater. Des.* **2001**, *22*, 123.
5. Macciniuc, A.; Rochette, A.; Rodrigue, D. *Prog. Rubber Plast. Recycl.* **2012**, *28*, 43.
6. Obrecht, W.; Lambert, J.-P.; Happ, M.; Oppenheimer-Stix, C.; Dunn, J.; Krüger, R. In *Ullmann's Encyclopedia of Industrial Chemistry*, 7th ed.; Wiley-VCH: Weinheim, **2010**; p 623.
7. Sardashti, M.; Gislason, J. J.; Lai, X.; Stewart, C. A.; O'Donnell, D. *J. Appl. Spectrosc.* **2001**, *55*, 467.
8. Luo, H.; Klüppel, M.; Schneider, H. *Macromolecules* **2004**, *37*, 8000.
9. Arantes, T. M.; Leão, K. V.; Tavares, M. I. B.; Ferreira, A. G.; Longo, E.; Camargo, E. R. *Polym. Test.* **2009**, *28*, 490.
10. Kawahara, S.; Chaikumpollert, O.; Sakurai, S.; Yamamoto, Y.; Akabori, K. *Polymer* **2009**, *50*, 1626.
11. Nakazono, T.; Matsumoto, A. *J. Appl. Polym. Sci.* **2010**, *118*, 2314.
12. Liang, H.; Hardy, J.-M.; Rodrigue, D.; Brisson, J. *Rubber Chem. Technol.* **2014**, *87*, 538.
13. Shield, S. R.; Ghebremeskel, G. N. *Rubber World* **2000**, *223*, 25.
14. Castaldi, M. J.; Kwon, E. In *13th North American Waste to Energy Conference*, Orlando, FL, 2005; p 19.
15. Fink, H.; Panne, U.; Theisen, M.; Niessner, R.; Probst, T.; Lin, X.; Fresenius, J. *Anal. Chem.* **2000**, *368*, 235.
16. Mans, C.; Hanning, S.; Simons, C.; Wegner, A.; Janßen, A.; Kreyenschmidt, M. *Spectrochim. Acta Part B* **2007**, *62*, 116.
17. Miskolczi, N.; Nagy, R.; Bartha, L.; Halmos, P.; Fazekas, B. *Microchem. J.* **2008**, *88*, 14.
18. Tertian, R.; Claisse, F. *Principles of Quantitative X-ray Fluorescence Analysis*; Heyden & Son: London, **1982**; p 317.
19. Radhakrishnan, C. K.; Sujith, A.; Unnikrishnan, G. *J. Therm. Anal. Calorim.* **2007**, *90*, 191.
20. Noriman, N. Z.; Ismail, H.; Rashid, A. A. *Polym. Test.* **2010**, *29*, 200.
21. Arockiasamy, A.; Toghiani, H.; Oglesby, D.; Horstemeyer, M. F.; Bouvard, J. L.; King, R. *J. Therm. Anal. Calorim.* **2013**, *111*, 535.
22. Hertz, D. L. *Elastomerics* **1984**, *116*, 1721.
23. Amari, T.; Themelis, N. J.; Wernick, I. K. *Resour. Policy* **1999**, *25*, 179.
24. Cunliffe, A. M.; Williams, P. T. *Environ. Technol.* **1998**, *19*, 1177.
25. Metz, U.; Hoffmann, P.; Weinbruch, S.; Ortner, H. *Mikrochim. Acta* **1994**, *117*, 95.
26. Mans, C.; Simons, C.; Hanning, S.; Janßen, A.; Alber, D.; Radtke, M.; Reinholz, U.; Bühler, A.; Kreyenschmidt, M. *X-Ray Spectrom.* **2009**, *38*, 52.
27. Mellawati, J.; Sumarti, M.; Menry, Y.; Surtipanti, S.; Kump, P. *Appl. Radiat. Isot.* **2001**, *54*, 881.
28. Choi, S.-S.; Kim, Y.; Kwon, H.-M. *RSC Adv.* **2014**, *4*, 31113.

29. Koval'aková, M.; Fričová, O.; Hronský, V.; Olčák, D.; Mandula, J.; Salaiová, B. *Road Mater. Pavement* **2013**, *14*, 946.
30. Zhang, A.; Chao, L. *Eur. Polym. J.* **2003**, *39*, 1291.
31. Rodgers, B.; Waddell, W. In *The Science and Technology of Rubber*, 4th ed.; Mark, J. E.; Erman, B.; Roland, M., Eds.; Academic Press: San Diego, CA, **2013**; p 650.
32. Jimenez, A.; Lopez, J.; Torre, L.; Kenny, J. M. *J. Appl. Polym. Sci.* **1999**, *73*, 1069.
33. Sircar, A. K. *Rubber Chem. Technol.* **1992**, *65*, 503.
34. Fernández-Berridi, M. J.; González, N.; Mugica, A.; Bernicot, C. *Thermochim. Acta* **2006**, *444*, 65.
35. Kraus, G.; Childers, C. W.; Gruver, J. T. *J. Appl. Polym. Sci.* **1967**, *11*, 1581.
36. Chapman, A. V.; Tinker, A. J.; Brickendonbury, H. J. *Elast. Plast.* **2003**, *56*, 533.
37. Andrews, R. J.; Grulke, E. A.; Glass Transition Temperatures of Polymers. Wiley Database of Polymer Properties. Wiley: Hoboken, 2003; Chapter 5. <http://onlinelibrary.wiley.com/doi/10.1002/0471532053.bra039/full>.